MOLECULAR AND CELLULAR BIOLOGY, Aug. 2006, p. 6157–6169 Vol. 26, No. 16
0270-7306/06/$08.00+0 doi:10.1128/MCB.00595-06

Fbxw8 Is Essential for Cul1-Cul7 Complex Formation and for Placental Development

Ryosuke Tsunematsu,[1,2] Masaaki Nishiyama,[1,2] Shuhei Kotoshiba,[1,2] Toru Saiga,[1,2] Takumi Kamura,[1,2] and Keiichi I. Nakayama[1,2]*

Department of Molecular and Cellular Biology, Medical Institute of Bioregulation, Kyushu University, Fukuoka 812-8582,[1] and CREST, Japan Science and Technology Agency, Kawaguchi, Saitama 332-0012,[2] Japan

Received 6 April 2006/Returned for modification 22 May 2006/Accepted 6 June 2006

Cullin-based ubiquitin ligases (E3s) constitute one of the largest E3 families. Fbxw8 (also known as Fbw6 or Fbx29) is an F-box protein that is assembled with Cul7 in an SCF-like E3 complex. Here we show that Cul7 forms a heterodimeric complex with Cul1 in a manner dependent on Fbxw8. We generated mice deficient in Fbxw8 and found that Cul7 did not associate with Cul1 in cells of these mice. Two-thirds of *Fbxw8*$^{-/-}$ embryos die in utero, whereas the remaining one-third are born alive and grow to adulthood. *Fbxw8*$^{-/-}$ embryos show intrauterine growth retardation and abnormal development of the placenta, characterized by both a reduced thickness of the spongiotrophoblast layer and abnormal vessel structure in the labyrinth layer. Although the placental phenotype of *Fbxw8*$^{-/-}$ mice resembles that of *Cul7*$^{-/-}$ mice, other abnormalities of *Cul7*$^{-/-}$ mice are not apparent in *Fbxw8*$^{-/-}$ mice. These results suggest that the Cul7-based SCF-like E3 complex has both Fbxw8-dependent and Fbxw8-independent functions.

Ubiquitin-dependent proteolysis plays indispensable roles in various biological processes (6, 17, 38). Protein ubiquitylation is mediated by several enzymes that act in concert. A ubiquitin-activating enzyme (E1), with ATP as a substrate, catalyzes the formation of a thioester bond between itself and ubiquitin, and it then transfers the activated ubiquitin to a ubiquitin-conjugating enzyme (E2). Certain E2 enzymes transfer ubiquitin directly to the protein substrate, whereas others require the participation of a third component, a ubiquitin ligase (E3), to achieve this effect (16). Hundreds of E3s have been identified in eukaryotes and classified into three groups: HECT-type, U-box-type, and RING-type E3s. Cullin-based E3s, a subtype of RING-type E3s, are multisubunit complexes (13, 30). To date, seven mammalian proteins, Cul1, Cul2, Cul3, Cul4A, Cul4B, Cul5, and Cul7, have been identified as members of the cullin family. These proteins interact via their COOH-terminal cullin homology domain with Rbx1 or Rbx2, each of which contains a RING finger domain that interacts with E2. They also interact via their NH_2-terminal cullin repeat (with or without the participation of an adapter molecule such as Skp1 or Elongin C) with substrate recognition molecules, such as F-box proteins in the Cul1-based SCF complex (7, 20, 23, 28, 39), VHL-box proteins in the Cul2-based ECV complex (22), BTB domain proteins in the Cul3-based E3 complex (12, 31, 40), and SOCS-box proteins in the Cul5-based ECS complex (22). At least two other molecules, the APC2 subunit of the anaphase-promoting complex/cyclosome and the Cul7-related protein Parc, also possess a cullin homology domain (30, 34).

Cul7 was originally identified as p185, a protein that binds the large T antigen of simian virus 40 (24). The interaction of p185 with large T antigen is important for the cellular transformation activity of the latter (2), and the BH3 domain identified in the COOH-terminal region of p185 is thought to function in the promotion of apoptosis (36). More recently, p185 was isolated as a protein that binds Rbx1 and which contains a COOH-terminal cullin homology domain; it was thus named Cul7 (11). Cul7 possesses ubiquitylation activity in vitro and interacts with the F-box protein Fbxw8 (also known as Fbw6 or Fbx29), which was identified as a Cul7-binding protein by "pull-down" analysis with Cul7 (11). Fbxw8 is thus not only the receptor component of an SCF (Skp1, Cul1, F-box protein, Rbx1)-type E3 complex but is also the only F-box protein known to interact with Cul7 (4, 11). Cul7 does not interact directly with Skp1 but does so indirectly in an Fbxw8-dependent manner. Fbxw8 appears to interact with Cul7 with a higher affinity than it does with Cul1.

Mice deficient in Cul7 exhibit intrauterine growth retardation as a result of abnormal development of the placenta, characterized by impaired formation of the spongiotrophoblast layer and of vessels in the labyrinth layer, and they die from respiratory distress soon after birth (4). In addition, Fbxw8 is unstable, and its expression is reduced to below detectable levels in *Cul7*$^{-/-}$ cells, with this phenotype being normalized by forced expression of exogenous Cul7. Cul7 is thus thought to play an important role in stabilization of Fbxw8 as well as in the normal development of the placenta and embryo. *Cul7* mutations were recently identified in several pedigrees of 3-M syndrome, an autosomal recessive form of hereditary dwarfism characterized by pre- and postnatal growth retardation without mental or endocrine disorders, suggesting that Cul7 is also indispensable for normal human growth (18).

It has remained unclear whether Fbxw8 is the only substrate recognition subunit of the Cul7-based SCF-like complex. To reveal the physiological roles of Fbxw8 and its corresponding E3 complexes, we have generated mice deficient in this protein. We now show that the phenotype of *Fbxw8*$^{-/-}$ mice is

* Corresponding author. Mailing address: Department of Molecular and Cellular Biology, Medical Institute of Bioregulation, Kyushu University, 3-1-1 Maidashi, Higashi-ku, Fukuoka 812-8582, Japan. Phone: 81-92-642-6815. Fax: 81-92-642-6819. E-mail: nakayak1@bioreg.kyushu-u.ac.jp.

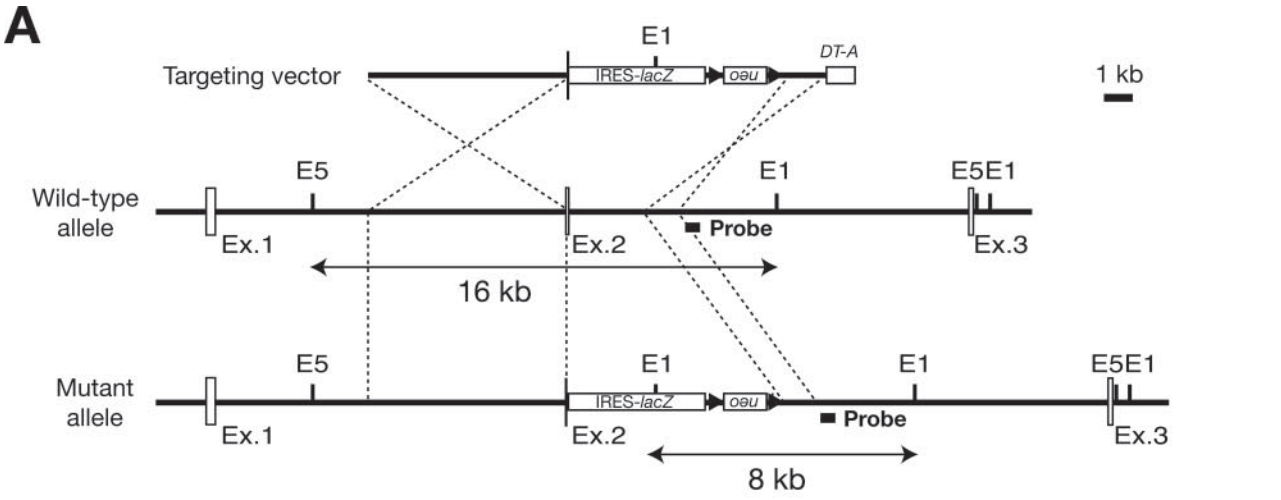
A
Targeting vector
E1
IRES-lacZ
DT-A
1 kb
Wild-type allele
E5
E1
E5E1
Ex.1
Ex.2
Ex.3
Probe
16 kb
Mutant allele
8 kb

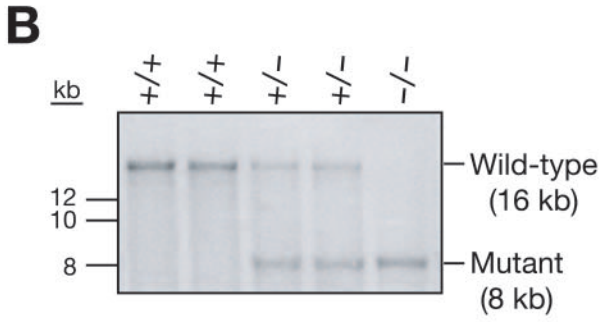
B
kb
+/+
+/+
+/−
+/−
−/−
12
10
8
Wild-type (16 kb)
Mutant (8 kb)

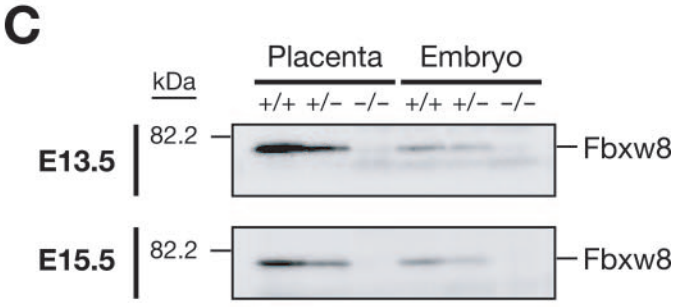
C
Placenta
Embryo
kDa
+/+ +/− −/− +/+ +/− −/−
E13.5
E15.5
82.2
Fbxw8

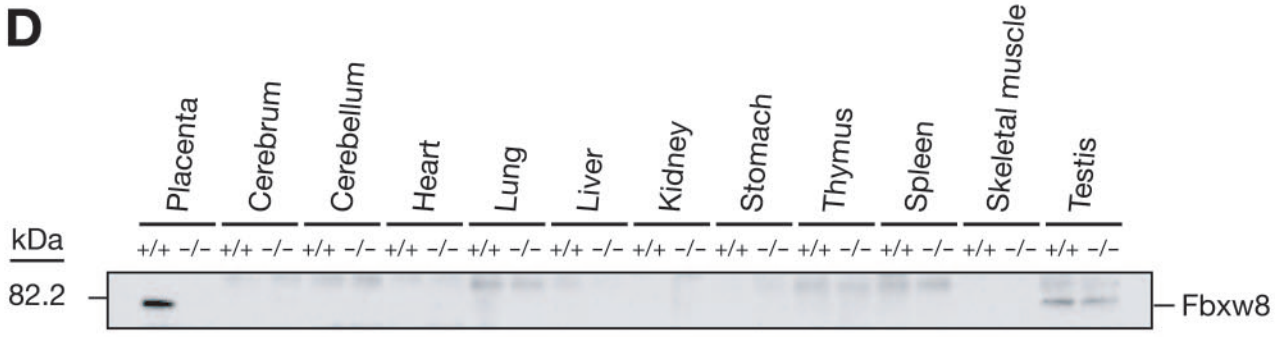
D
Placenta
Cerebrum
Cerebellum
Heart
Lung
Liver
Kidney
Stomach
Thymus
Spleen
Skeletal muscle
Testis
kDa
+/+ −/−
82.2
Fbxw8

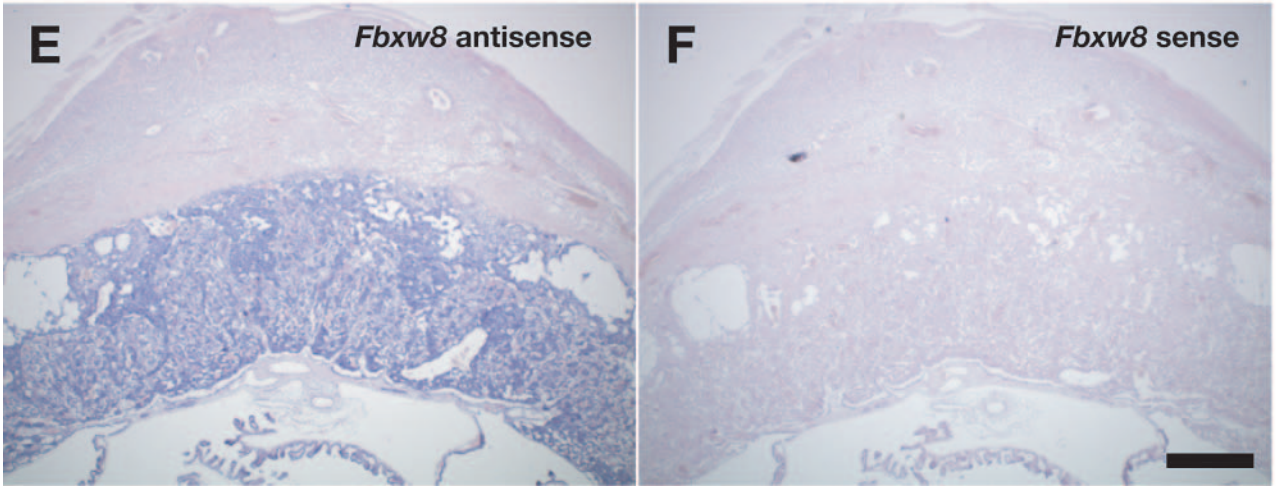
E
Fbxw8 antisense
F
Fbxw8 sense

similar to that of *Cul7*$^{-/-}$ mice, especially with regard to growth retardation and placental abnormality. However, other characteristics of *Cul7*$^{-/-}$ mice are not apparent in *Fbxw8*$^{-/-}$ mice, suggesting that the Cul7-based SCF-like complex has both Fbxw8-dependent and Fbxw8-independent functions. Moreover, we found that Cul7 forms a complex with Cul1 in an Fbxw8-dependent manner. Our data thus suggest that the newly identified Cul1-Fbxw8-Cul7 complex plays an important role in the normal development of the placenta.

MATERIALS AND METHODS

Generation of *Fbxw8*$^{-/-}$ mice. Cloned DNA corresponding to the *Fbxw8* locus was amplified from the genome of embryonic day 14 (E14) mouse embryonic stem (ES) cells with the use of LA-*Taq* polymerase (TaKaRa). The targeting vector was constructed by replacement of a 2.4-kb fragment of genomic DNA containing exon 2 of *Fbxw8* with IRES-*lacZ* and PGK-*neo*-poly(A)-loxP cassettes (5). The vector thus contained 6.5- and 1.2-kb regions of homology located 5′ and 3′, respectively, relative to IRES-*lacZ* and the neomycin resistance gene (*neo*). The diphtheria toxin A (DT-A) cassette was ligated at the 3′ end of the targeting construct. Maintenance, transfection, and selection of ES cells were performed as described previously (26). The recombination event was confirmed by Southern blot analysis with a 0.5-kb fragment of genomic DNA that flanks the 3′ homology region (Fig. 1A). The expected sizes of hybridizing fragments after digestion of genomic DNA with EcoRI and EcoRV are 16 and 8 kb for the wild-type and mutant *Fbxw8* alleles, respectively. Mutant ES cells were microinjected into C57BL/6 blastocysts, and resulting male chimeras were mated with female C57BL/6 mice. The germ line transmission of the mutant allele was confirmed by Southern blot analysis. Heterozygous offspring were intercrossed to produce homozygous mutant animals and their littermate controls. For genotyping of embryos, DNA was extracted from the yolk sac or tail at E11.5 to E19.5 and analyzed by PCR with the primers RT259 (5′-TCCCAGTGTGTGTGCATGTGTGAG-3′), RT260 (5′-GATGATGGAAACCAAGCCAATGC-3′), and PJL (5′-TGCTAAAGCGCATGCTCCAGACTGT-3′). All mouse experiments were approved by the animal ethics committee of Kyushu University.

Antibodies. Polyclonal anti-Fbxw8, anti-Cul7, and anti-Rbx1 antibodies were generated in rabbits with a recombinant COOH-terminal fragment of mouse Fbxw8, a recombinant NH_2-terminal fragment of mouse Cul7, and recombinant human full-length Rbx1 produced in *Escherichia coli*. Polyclonal anti-Cul1 antibodies were obtained from Zymed, monoclonal anti-Skp1 and anti-HSP70 antibodies were from BD Transduction Laboratories, and monoclonal anti-FLAG (M2) antibody was from Sigma.

Histological analysis. Tissue was fixed with 4% paraformaldehyde in phosphate-buffered saline, embedded in paraffin, and sectioned at a thickness of 3 μm. Hematoxylin-eosin staining was performed as described previously (27). Sixteen different fields (magnification, ×200) were randomly selected for measurement of the mean areas of maternal and fetal vessels in the placenta with the use of SCION Image software. For immunofluorescence, samples were fixed with 4% paraformaldehyde in phosphate-buffered saline, embedded in OCT compound (Tissue Tek), and sectioned with a cryostat at a thickness of 5 μm. Immunohistofluorescence analysis was performed as described previously (27, 37) with monoclonal anti-PECAM-1 (MEC13.3; PharMingen) and polyclonal anti-cytokeratin (WSS; Dako). Immune complexes were detected with secondary antibodies labeled with Alexa 546 or Alexa 488 (each at a 1:2,000 dilution). The specimens were examined with a fluorescence microscope and photographed.

In situ hybridization. Tissue was fixed with 4% paraformaldehyde in phosphate-buffered saline, embedded in paraffin, and sectioned at a thickness of 5 μm. Riboprobes specific for Fbxw8 or Tpbp mRNAs were synthesized with a DIG RNA labeling kit (Roche). In situ hybridization was performed with the Ventana HX system as described previously (37). Sections were counterstained with Nuclear Fast Red (Ventana).

Preparation of MEFs. Primary mouse embryonic fibroblasts (MEFs) were obtained from E13.5 embryos and cultured as previously described (26). For biochemical analysis, the cells were plated in 10-cm dishes at a density of 2×10^6 cells per dish.

Plasmids, transfection, immunoprecipitation, and immunoblot analysis. Mouse cDNAs for Fbxw5, Fbxw8, and Fbxw8 deletion mutants were subcloned into the p3xFLAG-CMV 7.1 vector (Sigma). HEK293T cells were transfected with the resulting plasmids by the calcium phosphate method and cultured for 48 h before analysis. For retrovirus production, full-length mouse Cul1, Cul2, and Cul7 cDNAs were each subcloned into the pMX-puro II-U6-3xFLAG vector (21). The resulting plasmids were introduced into Plat-E cells by transfection with the Fu-Gene reagent (Roche) to generate recombinant retroviruses. MEFs were infected with the recombinant retroviruses and subjected to selection for 3 days in medium containing puromycin (10 μg/ml). The surviving cells were then isolated, lysed in a solution containing 0.5% Triton X-100, and subjected to immunoprecipitation with anti-FLAG as described previously (15). Embryos, placenta, and adult mouse tissue samples were lysed in radioimmunoprecipitation assay buffer and subjected to immunoprecipitation and immunoblot analysis as described previously (27, 37).

RNA interference (RNAi). The pMX-puro II-U6/shRNA vector was constructed as described previously (21). The DNA for the short hairpin RNA (shRNA) encoded a 21-nucleotide hairpin sequence specific to the mRNA target, with a loop sequence (5′-TTCAAGAGA-3′) separating the two complementary domains, and it contained a tract of five T nucleotides to terminate transcription. The hairpin sequences specific for mouse Cul7 (mCul7-1 and mCul7-2) and enhanced green fluorescent protein (EGFP; Clontech) mRNAs corresponded to nucleotides 3022 to 3042 (mCul7-1), 4714 to 4734 (mCul7-2), and 126 to 146 (EGFP) of the respective coding regions. Recombinant retroviruses were produced and used to infect MEFs as described above. After selection in medium containing puromycin (10 μg/ml), cells stably expressing the shRNA were pooled for experiments.

RESULTS

To elucidate the physiological functions of Fbxw8, we generated mice deficient in this protein. The *Fbxw8* gene was disrupted in mouse embryonic stem cells by replacement of exon 2, which encodes the NH_2 terminus of Fbxw8, with IRES-*lacZ* and PGK-*neo*-poly(A)-loxP cassettes (Fig. 1A). We verified the homologous recombination by Southern blot analysis of the resulting mutant embryos (Fig. 1B). Immunoblot analysis also revealed that Fbxw8 was not detectable in homozygous mutant embryos or in the corresponding placentas (Fig. 1C). Although the abundance of Fbxw8 in heterozygous mice was about half of that in wild-type animals, the heterozygotes appeared normal and were healthy and fertile. The ratio of heterozygous to wild-type offspring produced from *Fbxw8*$^{+/-}$ intercrosses was also normal, whereas the number of *Fbxw8*$^{-/-}$ offspring was approximately one-third of that predicted by

FIG. 1. Targeting of *Fbxw8* and expression of Fbxw8. (A) Schematic representation of the wild-type *Fbxw8* locus, the targeting vector, and the mutant allele after homologous recombination. A 2.4-kb genomic fragment including exon 2 of *Fbxw8*, which encodes the F-box domain, was replaced by IRES-*lacZ* and PGK-*neo*-poly(A)-loxP cassettes. Exons (Ex.) and the probe used for Southern hybridization are denoted by open and filled boxes, respectively. Restriction sites: E1, EcoRI; E5, EcoRV. DT-A, diphtheria toxin A cassette. (B) Southern blot analysis with the probe shown in panel A of genomic DNA from E15.5 embryos after its digestion with EcoRI and EcoRV. The 16- and 8-kb bands corresponding to the wild-type and mutant alleles, respectively, are indicated. The *Fbxw8* genotypes of the embryos are shown above each lane. (C and D) Immunoblot analysis with anti-Fbxw8 of immunoprecipitates prepared with anti-Fbxw8 from lysates both of E13.5 and E15.5 embryos and placentas (C) and of tissues from adult mice of the indicated *Fbxw8* genotypes (D). (E and F) In situ hybridization analysis of the placenta of a wild-type embryo at E12.5 with a riboprobe specific for Fbxw8 mRNA (left panel). A control hybridization with the corresponding sense probe was also performed (right panel). *Fbxw8* is expressed in trophoblast lineage cells of the placenta. Scale bar, 500 μm.

TABLE 1. Genotype frequencies of embryos and live offspring produced from *Fbxw8*$^{+/-}$ intercrosses

Embryonic day	No. of animals recoverable[a]			
	+/+	+/−	−/−	Total
11.5	13	20	20	53
12.5	30	62	23 (1)	115 (1)
13.5	38	72	26 (2)	136 (2)
15.5	27	49	13 (5)	89 (5)
17.5	16	33	6 (1)	55 (1)
Adult	97	186	29	312

[a] Numbers in parentheses indicate resorbed embryos.

Mendel's law (Table 1), suggesting that the mutation is partially embryonic lethal in the homozygous state.

Immunoblot analysis of wild-type mice with antibodies to Fbxw8 also revealed that Fbxw8 was more abundant in the placenta than in the embryo at embryonic day 13.5 (Fig. 1C), and that it was not detectable in any of the adult tissues examined (Fig. 1D). (The band yielded by the testis that migrates at a position slightly above that of Fbxw8 appears to be nonspecific, given that it was observed for both wild-type and *Fbxw8*$^{-/-}$ genotypes.) In situ hybridization with a riboprobe specific for Fbxw8 mRNA showed that the mRNA was present in the trophoblast layer but not in the decidual layer of the E12.5 placenta (Fig. 1E). These data suggested that Fbxw8 might play an important role in placental development.

We examined embryos from *Fbxw8*$^{+/-}$ intercrosses at various developmental stages to determine the time at which *Fbxw8*$^{-/-}$ embryos become abnormal. All *Fbxw8*$^{-/-}$ embryos were still recoverable at E11.5, whereas some of them were already dead or had begun to degenerate by E12.5 (Table 1). The number of live *Fbxw8*$^{-/-}$ embryos was reduced to about one-half of that of wild-type littermates by E15.5. Growth retardation of homozygous mutant embryos and a reduction in size of the corresponding placentas were also apparent as early as E12.5 but became more obvious at later stages of gestation (Fig. 2A). The intrauterine growth retardation of *Fbxw8*$^{-/-}$ embryos was reminiscent of that apparent for *Cul7*$^{-/-}$ mice (4). About two-thirds of *Fbxw8*$^{-/-}$ embryos eventually died in utero, with the remaining one-third being born alive. The *Fbxw8*$^{-/-}$ neonates were smaller than their wild-type littermates, however, and remained so throughout postnatal life (Fig. 2B). No other gross abnormality was apparent in adult *Fbxw8*$^{-/-}$ mice, and these animals did not die prematurely or show predisposition to cancer.

Given that *Cul7*$^{-/-}$ neonates die soon after birth from respiratory failure as a result of a failure of the lungs to inflate (4), we examined the lungs of *Fbxw8*$^{-/-}$ fetuses at E19.5. The lungs of the mutant fetuses inflated as well as did those of their wild-type littermates (data not shown), suggesting that the lung phenotype of *Cul7*$^{-/-}$ mice is independent of Fbxw8. We also examined the proliferation of MEFs prepared from E13.5 embryos and did not find any substantial difference between the *Fbxw8*$^{-/-}$ and wild-type cells, although the growth of the mutant MEFs tended to be slightly slower than that of the *Fbxw8*$^{+/+}$ cells (data not shown). MEFs derived from *Cul7*$^{-/-}$ embryos exhibit a significant growth defect in culture (4).

The placenta of *Fbxw8*$^{-/-}$ embryos is grossly abnormal (Fig. 2A). The mouse placenta comprises four layers: the decidual layer, trophoblast giant cell layer, spongiotrophoblast layer, and labyrinth layer (1, 32). Hematoxylin-eosin staining of the placenta of E12.5 embryos revealed that the border of the spongiotrophoblast layer and labyrinth layer was unclear in the *Fbxw8*$^{-/-}$ placenta, whereas the decidual and trophoblast giant cell layers of the *Fbwx8*$^{-/-}$ placenta appeared normal (Fig. 3A and B). Similar differences between the placentas of wild-type and mutant embryos were also apparent at later gestational stages (data not shown). The placenta of some *Fbxw8*$^{-/-}$ embryos also manifested irregular dilation of vessels in the labyrinth layer (Fig. 3B). In situ hybridization analysis of the mRNA for the spongiotrophoblast-specific marker Tpbp (1, 4) also revealed that the spongiotrophoblast layer of the *Fbxw8*$^{-/-}$ placenta was reduced in thickness compared with that of the wild-type placenta (Fig. 3C and D). Irregular protrusion of spongiotrophoblasts into the labyrinth layer was also observed in the placenta of mutant embryos (Fig. 3D). Expression of the gene for PL-1, a marker for trophoblast giant cells (1), and of that for GCM1, a marker for the labyrinth layer (3), did not appear to be affected by the *Fbxw8* mutation (data not shown). Immunohistofluorescence staining of the placenta of wild-type and *Fbxw8*$^{-/-}$ embryos with antibodies to cytokeratin, a marker for trophoblast lineage cells in the spongiotrophoblast and labyrinth layers, and with antibodies to PECAM-1, a marker for endothelial cells in the labyrinth layer, yielded results consistent with those of in situ hybridization analysis of Tpbp mRNA (Fig. 4). These various data thus indicate that development of the spongiotrophoblast layer is impaired in *Fbxw8*$^{-/-}$ mice.

Vessels in the labyrinth layer are also abnormal in *Cul7*$^{-/-}$ mice (4). We measured the areas of maternal and fetal vessels in the labyrinth layer of the placenta of wild-type and *Fbxw8*$^{-/-}$ embryos. Maternal and fetal vessels were distinguished from each other on the basis of the presence of nucleated (fetal) or denucleated (maternal) red blood cells. Similar to *Cul7*$^{-}$/$^{-}$ mice, the maternal vessel area of the *Fbxw8*$^{-/-}$ placenta was significantly smaller than that of the wild-type placenta (Fig. 3E). The fetal vessel area of the *Fbxw8*$^{-/-}$ placenta tended to be larger than that of the wild-type placenta, but this difference was not statistically significant. These observations suggest that development of the labyrinth layer is also defective in *Fbxw8*$^{-/-}$ mice, resulting in an imbalance in the feto-maternal circulation.

To investigate whether the maternal *Fbxw8* mutation affected the placental phenotype of *Fbxw8*$^{-/-}$ embryos, we compared crosses of *Fbxw8*$^{+/-}$ females and *Fbxw8*$^{+/-}$ males with those of *Fbxw8*$^{-/-}$ females and *Fbxw8*$^{+/-}$ males (Fig. 5). (All other analyses in this study were performed with embryos produced from *Fbxw8*$^{+/-}$ intercrosses.) Histological analysis of the placenta in pregnant females revealed that those of *Fbxw8*$^{+/+}$ and *Fbxw8*$^{+/-}$ embryos developed normally, whereas that of *Fbxw8*$^{-/-}$ embryos was defective, regardless of the maternal *Fbxw8* genotype. The placental phenotype thus depends solely on the fetal genotype.

Fbxw8 contains an F-box domain in its NH_2-terminal region and five WD40 domains in its central and COOH-terminal regions (Fig. 6C). Fbxw8 was previously shown to bind to overexpressed Cul7 to a greater extent than to overexpressed Cul1 in transfected cells (4, 11). We examined the interactions

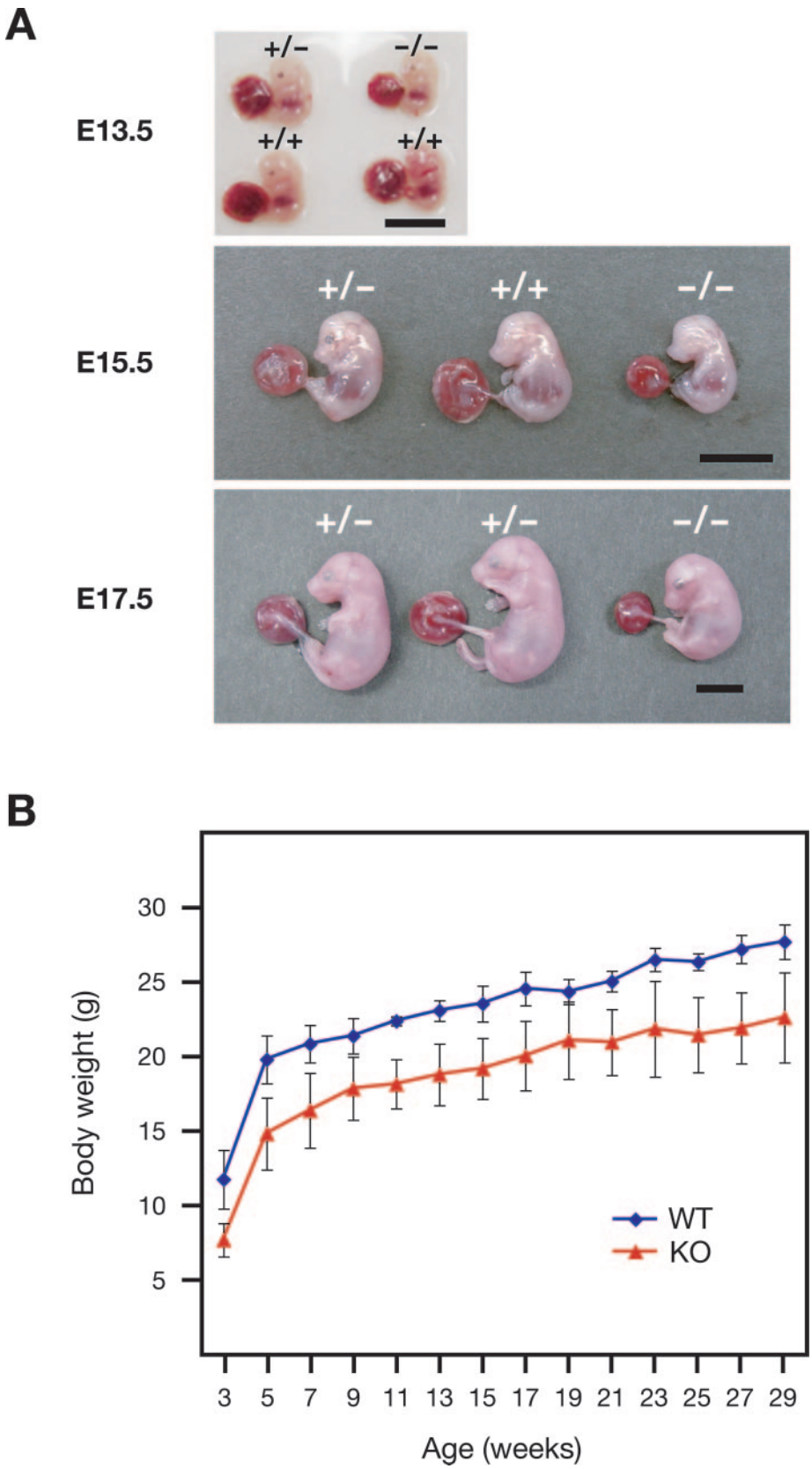

FIG. 2. Intrauterine growth retardation in *Fbxw8*$^{-/-}$ mice. (A) Gross appearance of littermates from *Fbxw8*$^{+/-}$ intercrosses at E13.5, E15.5, and E17.5. *Fbxw8*$^{-/-}$ embryos are smaller than their littermate controls and have smaller placentas, indicative of intrauterine growth retardation. Scale bars, 10 mm. (B) Time course of body weight gain of the *Fbxw8*$^{-/-}$ (KO) and wild-type (WT) offspring from *Fbxw8*$^{+/-}$ intercrosses. Data are means ± standard errors of the means for four mice of each genotype.

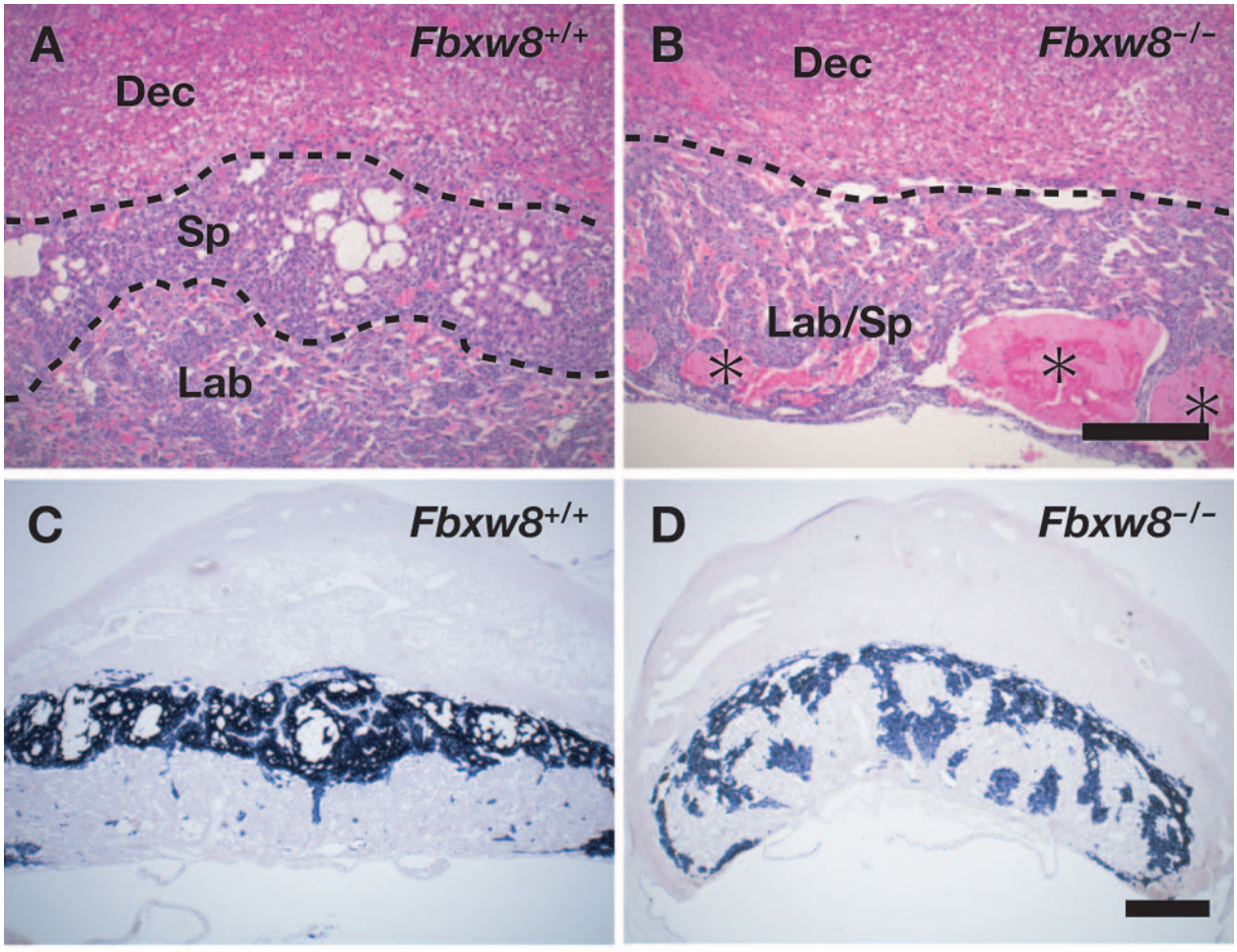
A
Fbxw8+/+
Dec
Sp
Lab
B
Dec
Fbxw8−/−
Lab/Sp
C
Fbxw8+/+
D
Fbxw8−/−
E
Fbxw8+/+
Fbxw8−/−
Fetal vessel area (%)
16
12
8
4
0
n.s.
WT
KO
Maternal vessel area (%)
20
15
10
5
0
p < 0.005
WT
KO

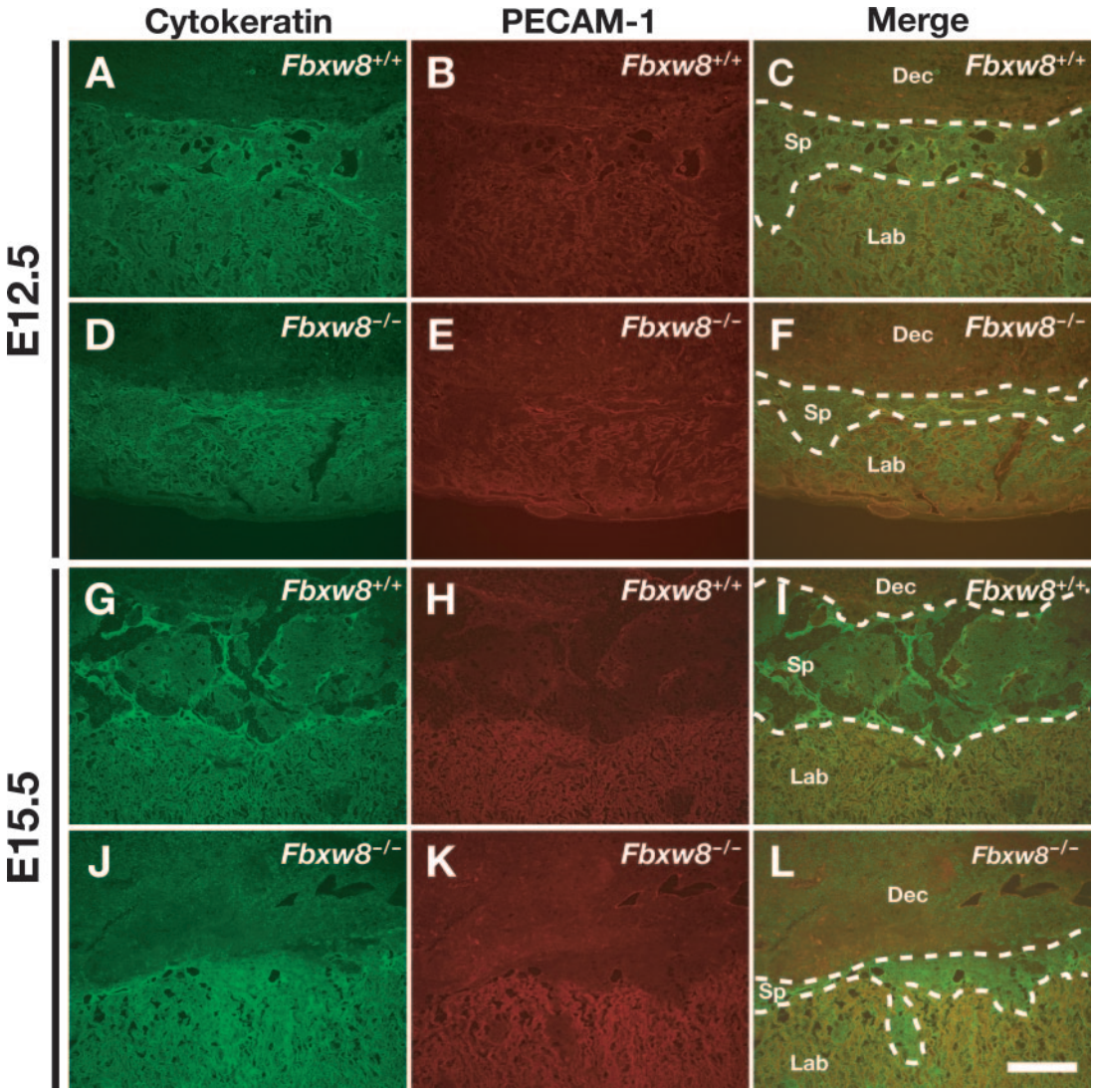

FIG. 4. Reduced thickness of the spongiotrophoblast layer in the placenta of *Fbxw8*$^{-/-}$ embryos. The placenta of wild-type (A to C as well as G and H) and *Fbxw8*$^{-/-}$ (D to F and J to L) embryos at E12.5 (A to F) or E15.5 (G to L) was subjected to immunohistofluorescence analysis with anti-cytokeratin (A, D, G, and J) and anti-PECAM-1 (B, E, H, and K). Merged images are shown (C, F, I, and L). Cytokeratin is expressed in trophoblast lineage cells, and PECAM-1 is expressed in vascular endothelial cells. The spongiotrophoblast layer is stained predominantly by anti-cytokeratin antibody, whereas the labyrinth layer is stained by both types of antibodies. The two types of staining in the labyrinth layer do not merge, because maternal vessels in this layer consist of trophoblast lineage cells and lack endothelial cells. The thickness of the spongiotrophoblast layer is markedly reduced in the placenta of *Fbxw8*$^{-/-}$ embryos. Dec, decidual layer; Sp, spongiotrophoblast layer; Lab, labyrinth layer. Scale bar, 300 μm.

among these endogenous proteins in lysates prepared from the placenta of *Fbxw8*$^{+/+}$ or *Fbxw8*$^{+/-}$ embryos. Coimmunoprecipitation analysis revealed that endogenous Fbxw8 interacts with both endogenous Cul1 and Cul7, as well as with Skp1 and Rbx1, in wild-type lysates (Fig. 6A). Such analysis also indicated that endogenous Fbxw8 did not bind endogenous Cul7 to a greater extent than it did endogenous Cul1. Similarly, overexpressed Fbxw8 did not seem to bind to endogenous Cul7

FIG. 3. Abnormal placental development in *Fbxw8*$^{-/-}$ mice. (A and B) Hematoxylin-eosin staining of the placenta of *Fbxw8*$^{+/+}$ and *Fbxw8*$^{-/-}$ embryos, respectively, at E12.5. Impaired development of the spongiotrophoblast layer (delineated by the dashed lines) and abnormally dilated vessels in the labyrinth layer (asterisks) are apparent in the mutant. Dec, decidual layer; Sp, spongiotrophoblast layer; Lab, labyrinth layer. Scale bar, 300 μm. (C and D) In situ hybridization analysis of Tpbp mRNA in the placenta of *Fbxw8*$^{+/+}$ and *Fbxw8*$^{-/-}$ embryos, respectively, at E12.5. The spongiotrophoblast layer of the placenta was thinner in the mutant than in the wild type. Scale bar, 500 μm. (E) Areas of maternal and fetal vessels in the placenta of *Fbxw8*$^{-/-}$ and wild-type embryos at E12.5. Placental sections were subjected to hematoxylin-eosin staining for detection of maternal vessels (containing denucleated red blood cells, in red) and fetal vessels (containing nucleated red blood cells, in blue), as shown in the upper panels. The areas of maternal and fetal vessels were measured by image analysis. Sixteen different fields (magnification, ×200) for each genotype [*Fbxw8*$^{+/+}$ (WT) and *Fbxw8*$^{-/-}$ (KO)] were randomly selected for analysis, and the means ± standard errors of the means of the percentage area of each vessel type in each field was calculated. n.s., not significant ($P > 0.05$, Student's *t* test). Scale bar, 150 μm.

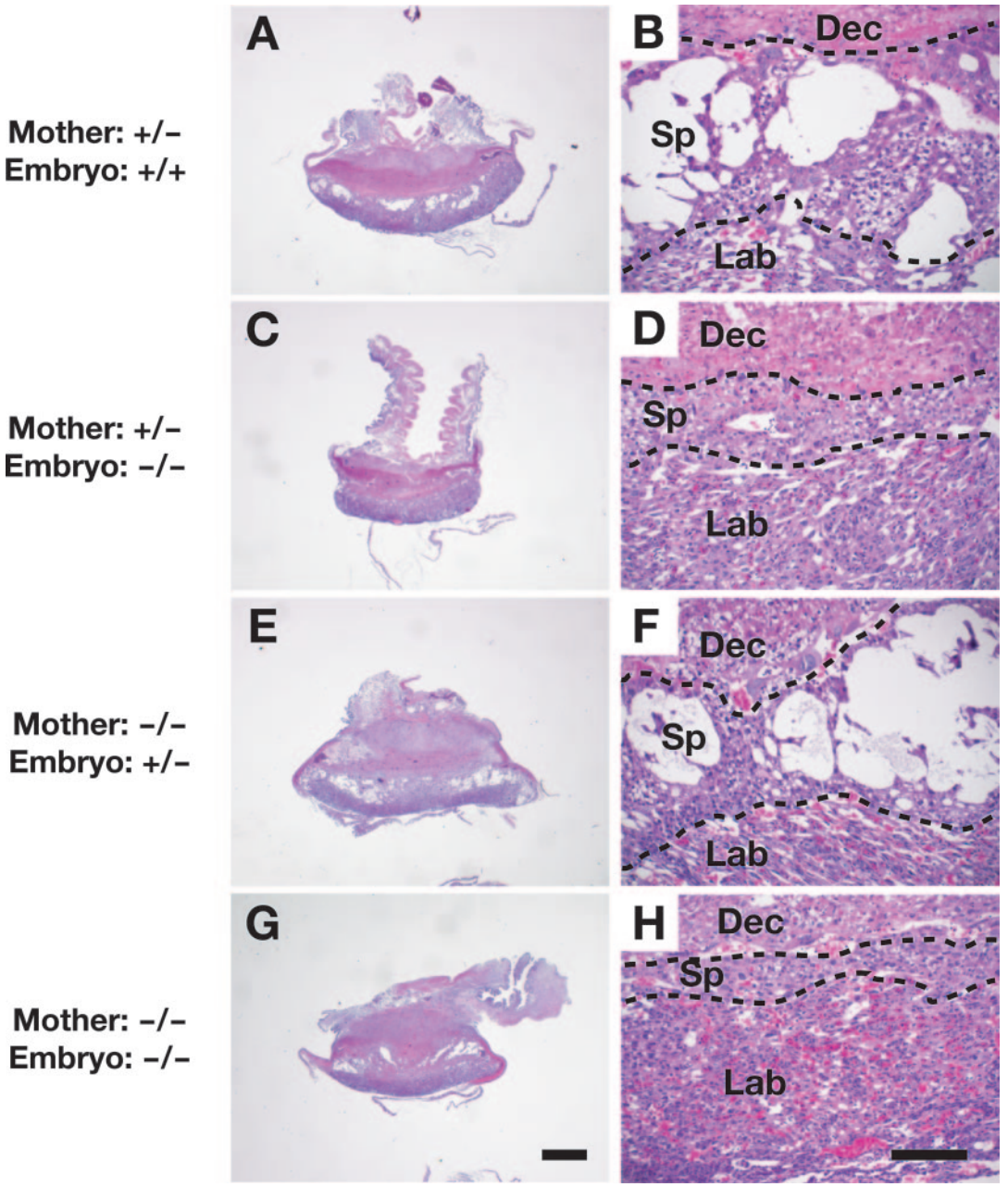

FIG. 5. Dependence of placental phenotype on *Fbxw8* genotype of the embryo. *Fbxw8*$^{+/-}$ and *Fbxw8*$^{-/-}$ females were crossed with *Fbxw8*$^{+/-}$ males, and the placenta of the resulting embryos at E12.5 was subjected to hematoxylin-eosin staining. The genotypes of mother and embryo are shown. The placenta of *Fbxw8*$^{-/-}$ embryos was smaller and exhibited a thinner spongiotrophoblast layer compared with that of *Fbxw8*$^{+/+}$ or *Fbxw8*$^{+/-}$ embryos regardless of maternal genotype. Dec, decidual layer; Sp, spongiotrophoblast layer; Lab, labyrinth layer. Scale bar, 1 mm (A, C, E, and G) or 300 μm (B, D, F, and H).

more strongly than it did to endogenous Cul1 (Fig. 6D). In the Fbxw8 immunoprecipitates prepared from the placenta of *Fbxw8*$^{+/-}$ embryos, however, the abundance of Cul1 and Skp1 was reduced in parallel with that of Fbxw8, whereas the amounts of Cul7 and Rbx1 appeared unaffected. These data suggested that Fbxw8 may associate preferentially with Cul7-Rbx1 rather than with the Skp1-Cul1-Rbx1 complex.

The abundance of Cul7 appeared normal in the placenta of *Fbxw8*$^{-/-}$ embryos (Fig. 6A), whereas Fbxw8 is too unstable to be detected in *Cul7*$^{-/-}$ mice (4). This latter finding is not the result of developmental bias due to gene inactivation, given that acute depletion of Cul7 by RNAi in wild-type MEFs also resulted in a marked reduction in the amount of Fbxw8 (Fig. 6B).

We investigated the regions of Fbxw8 that mediate the interactions with Cul1 and Cul7 by generating a series of deletion mutants of Fbxw8 tagged at their NH_2 termini with the 3× FLAG epitope (Fig. 6C). Lysates of HEK293T cells expressing

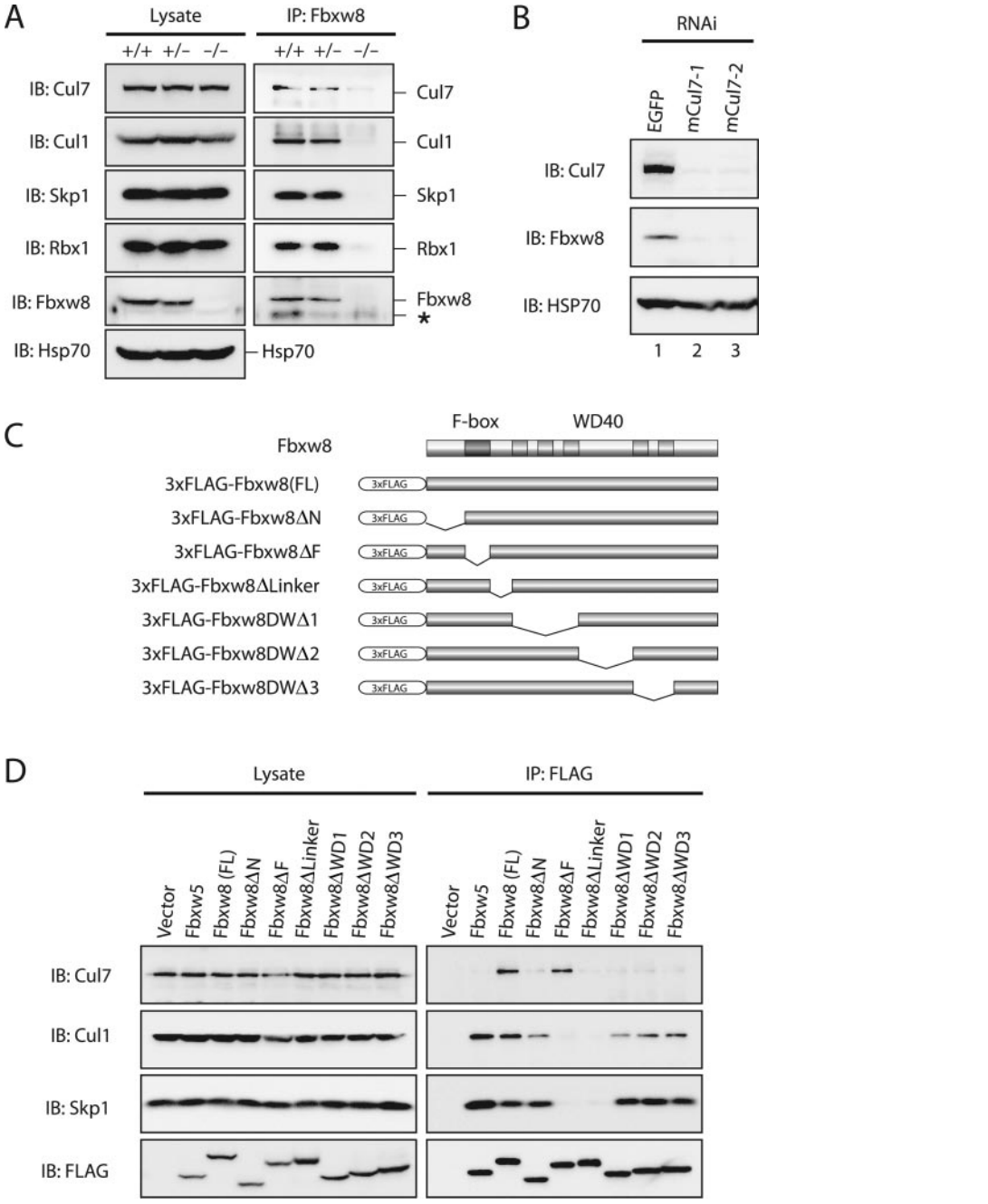

FIG. 6. Interactions between Fbxw8 and cullins. (A) Lysates of the placenta of E13.5 embryos of the indicated *Fbxw8* genotypes were subjected to immunoprecipitation (IP) with anti-Fbxw8, and the resulting precipitates as well as the original lysates were subjected to immunoblot (IB) analysis with antibodies to the indicated proteins. Asterisk indicates nonspecific bands. (B) Wild-type MEFs were infected with recombinant retroviruses encoding shRNAs specific for EGFP (control, lane 1) or Cul7 (lanes 2 and 3) mRNAs. Cell lysates were subsequently subjected to immunoblot analysis with antibodies to Cul7, Fbxw8, or HSP70 (control). (C) Schematic representation of Fbxw8 and 3× FLAG-tagged deletion mutants of Fbxw8. (D) Lysates of HEK293T cells expressing 3× FLAG-tagged Fbxw5, Fbxw8, or the deletion mutants of Fbxw8 shown in panel C were subjected to immunoprecipitation with anti-FLAG, and the resulting precipitates as well as the original cell lysates were subjected to immunoblot analysis with the indicated antibodies.

these various mutant proteins were then subjected to coimmunoprecipitation analysis with anti-FLAG (Fig. 6D). Full-length Fbxw8 interacted with both endogenous Cul1 and Cul7, whereas Fbxw5, another Fbxw-type F-box protein, associated with Cul1 but not with Cul7. A mutant of Fbxw8 that lacks the F-box domain (ΔF) retained the ability to interact with Cul7, but it failed to associate with Cul1. Conversely, deletion mutants that lack portions of the region of Fbxw8 containing the WD40 domains (ΔWD1, ΔWD2, or ΔWD3) or NH_2-terminal region (ΔN) failed to bind to Cul7 but retained the ability to

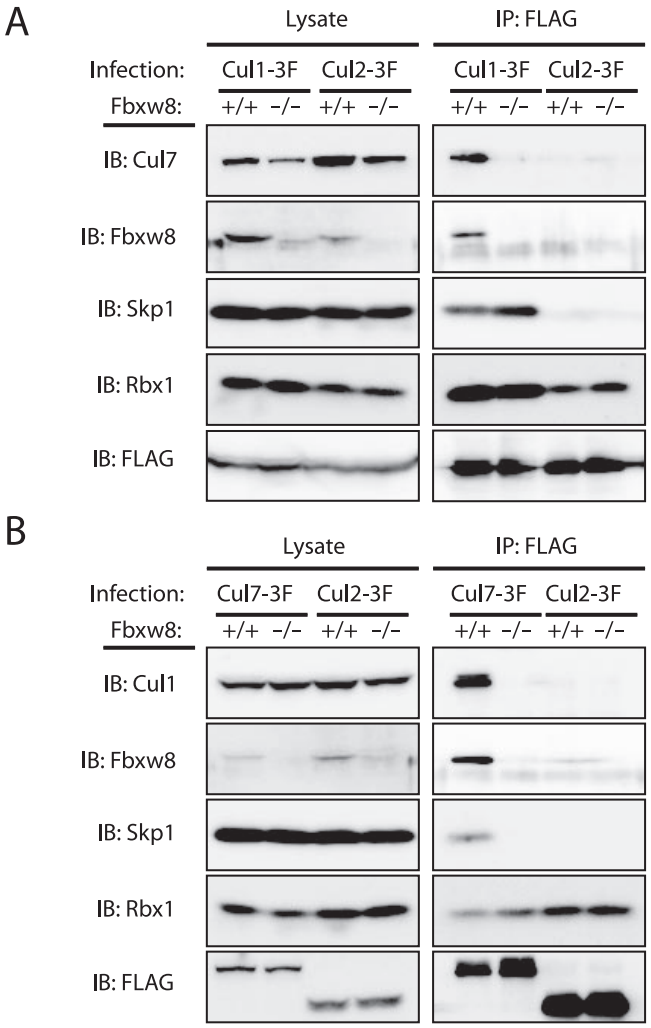

FIG. 7. Formation of a Cul1-Cul7 complex linked by Fbxw8. *Fbxw8*$^{+/+}$ or *Fbxw8*$^{-/-}$ MEFs were infected with recombinant retroviruses encoding 3× FLAG (3F)-tagged Cul1 (A) or Cul7 (B), and lysates of the infected cells were subjected to immunoprecipitation with anti-FLAG. The resulting precipitates as well as the original cell lysates were then subjected to immunoblot analysis with the indicated antibodies. Cells expressing 3× FLAG-Cul2 were also studied as a negative control. IB, immunoblot; IP, immunoprecipitation.

interact with Cul1. A deletion mutant that lacks the linker region (the region between the F-box domain and the first WD40 domain) did not interact with either Cul1 or Cul7. We also examined the binding of Skp1 to the Fbxw8 mutants and found that Skp1 bound to the same mutants as did Cul1. These results suggest that Fbxw8 binds to Cul1 via Skp1, as do other F-box proteins, whereas Fbxw8 interacts with Cul7 mainly through its central and COOH-terminal regions, not through its F-box domain, in an Skp1-independent manner.

Given that Fbxw8 interacts with both Cul1 and Cul7, we hypothesized that a single Fbxw8 molecule might bind to both Cul1 and Cul7 simultaneously. To test this hypothesis, we expressed 3× FLAG-tagged Cul1 in *Fbxw8*$^{+/+}$ or *Fbxw8*$^{-/-}$ MEFs and then subjected cell lysates to coimmunoprecipitation analysis with anti-FLAG (Fig. 7A). We also expressed 3× FLAG-tagged Cul2 as a control. Exogenous Cul1 formed a complex with endogenous Cul7 as well as with Fbxw8, Skp1, and Rbx1 in *Fbxw8*$^{+/+}$ MEFs, whereas the interaction between Cul1 and Cul7 was not detected in *Fbxw8*$^{-/-}$ MEFs. Exogenous Cul2 associated with neither Cul7 nor Skp1. To substantiate these results, we performed reciprocal coimmunoprecipitation experiments with MEFs expressing 3× FLAG-tagged Cul7 or Cul2 (Fig. 7B). Exogenous Cul7 interacted with Cul1 as well as with Fbxw8, Skp1, and Rbx1 in *Fbxw8*$^{+/+}$ MEFs. In contrast, the association of Skp1 and Cul1 with Cul7 was not detected in *Fbxw8*$^{-/-}$ MEFs. These results indicate that Cul7 forms a complex with Cul1 only in cells that express Fbxw8. In addition, both Cul1 and Cul7 bound to Rbx1 even in *Fbxw8*$^{-/-}$ cells in which the Cul1-Cul7 interaction was lost (Fig. 7), suggesting that both Cul1 and Cul7 interact with Rbx1 independently. Together with the results obtained with the deletion mutants of Fbxw8 (Fig. 6D), these data suggest that an Rbx1-Cul1-Skp1-Fbxw8-Cul7-Rbx1 complex forms in cells (Fig. 8). Furthermore, this complex likely plays an essential role in normal placental development.

DISCUSSION

Whereas the Cul1-based SCF complex has been extensively characterized, the structure and functions of the Cul7-based SCF-like complex have remained largely unknown. Compared with that of other cullins, the structure of Cul7 seems atypical. Whereas other cullins contain a binding domain for adapter proteins (such as Skp1 or Elongin C) juxtaposed NH_2 terminal to the cullin homology domain, Cul7 possesses a large region of unknown function NH_2 terminal to the cullin homology domain, except for a DOC domain at its central region. Immunoprecipitation and mass spectrometric analyses have revealed that the F-box protein Fbxw8 is present in the Cul7-based SCF-like complex (4, 11), although it has remained unknown whether Fbxw8 is the only substrate recognition subunit of this complex. Our genetic analysis now indicates that Cul7 has Fbxw8-independent functions, suggesting the existence of other such substrate recognition subunits (see below). Unexpectedly, we found that the F-box domain of Fbxw8 is not necessary for the interaction with Cul7, whereas it is required for the binding of Fbxw8 to Cul1. This finding is consistent with the previous observation that Skp1 is not necessary for the interaction between Cul7 and Fbxw8 (4, 11). These data thus indicate that Fbxw8 interacts with Cul7 in a manner independent of both the F-box domain and Skp1. Our binding data suggest that Cul7 associates directly or indirectly with the central and COOH-terminal regions of Fbxw8. The difference in the binding sites of Fbxw8 for Cul1 and Cul7 suggested the possibility that a Cul1-Fbxw8-Cul7 complex might form in cells. We have now demonstrated that such a complex indeed exists in wild-type cells, whereas Cul1 and Cul7 do not interact in *Fbxw8*$^{-/-}$ cells. We thus propose that Fbxw8 functions, at least in part, as a linker to tether Cul1 and Cul7 (Fig. 8).

Fbxw8 is unstable and undetectable in *Cul7*$^{-/-}$ mice (4). We have now shown that Fbxw8 is also undetectable in MEFs depleted of Cul7 by RNAi, suggesting that Cul7 plays a chaperone-like role in stabilizing Fbxw8 through formation of a stable Cul1-Fbxw8-Cul7 complex. In contrast, Cul7 expression was unaffected by the loss of Fbxw8 in the present study. The phenotype of *Cul7*$^{-/-}$ mice thus likely reflects the loss of

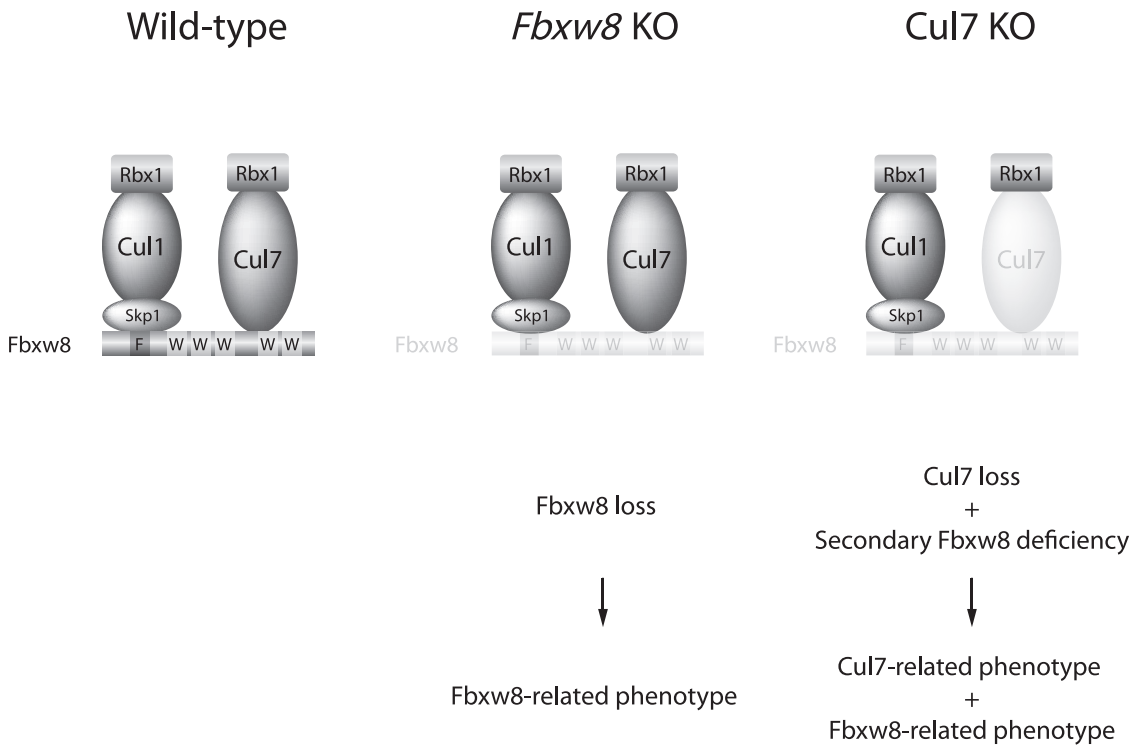

FIG. 8. Model for formation of a Cul1-Fbxw8-Cul7 complex. In wild-type mice, Cul7 associates with Cul1 via Fbxw8. In *Fbxw8*$^{-/-}$ (*Fbxw8* KO) mice, loss of Fbxw8 results in placental abnormalities (Fbxw8-related phenotype). In *Cul7*$^{-/-}$ mice, loss of Cul7 results in destabilization of Fbxw8 and consequent secondary loss of Fbxw8. *Cul7*$^{-/-}$ mice thus exhibit both the Fbxw8-related phenotype and a phenotype attributable to loss of Cul7 function not mediated by Fbxw8 (Cul7-related phenotype). F, F-box domain; W, WD40 repeat.

Fbxw8 function as well as the loss of Cul7 function that is independent of Fbxw8 (Fig. 8).

The Cul1-Fbxw8-Cul7 complex is likely to contain at least two molecules of Rbx1, which is thought to associate directly with the E2 Cdc34. To date, several types of E3 or E3 complex are known to contain two RING finger domains for E2 binding. For example, Parkin contains two RING finger domains (19, 29, 34), both of which are indispensable for its E3 activity (19). BRCA1 and BARD1, both of which contain a single RING finger domain, dimerize to exert E3 activity (14). These observations suggest that two RING finger domains might also be required for maximal activation of E3 activity in the Cul1-Fbxw8-Cul7 complex. In 3-M syndrome patients who harbor mutations in *Cul7*, some mutations are located in the exon that encodes the cullin homology domain and result in impaired binding to Rbx1 (18). In addition, F-box proteins such as mammalian β-TrCP1 and β-TrCP2 and *Schizosaccharomyces pombe* Pop1p and Pop2p form homo- or heterodimers to achieve efficient ubiquitylation of their substrate proteins or to generate combinatorial diversity (25, 33, 35), suggesting the possibility that Cul1 incorporated in the SCF complex might form a dimer through dimerization of F-box proteins. Cul7 also forms a dimer with the related protein Parc (34). These data suggest that cullin-based E3s generally exist as homo- or heterodimeric complexes.

The expression of Fbxw8 is largely restricted to the placenta, whereas Cul7 is expressed not only in the embryo and the placenta but also in various tissues of adult mice and humans (18, 36). A comparison of the phenotypes of *Fbxw8*$^{-/-}$ mice (this study) and *Cul7*$^{-/-}$ mice (4) is summarized in Table 2. Consistent with the tissue distributions of these proteins, the abnormalities in *Fbxw8*$^{-/-}$ mice appear to be restricted to the placenta, whereas those in *Cul7*$^{-/-}$ mice also involve other tissues. Both types of mice manifest abnormal development of the spongiotrophoblast and labyrinth layers of the placenta. During placental development, trophectodermal cells distant from the inner cell mass of the blastocyst stop dividing but undergo endoduplication of their DNA, resulting in the formation of polyploid trophoblast giant cells. Trophectodermal cells overlying the inner cell mass continue to proliferate to form extraembryonic ectoderm and the ectoplacental cone of the early postimplantation conceptus. After chorioallantoic fusion in the mouse at E8.5, chorionic ectodermal cells derived

TABLE 2. Comparison of phenotypes between *Fbxw8*$^{-/-}$ and *Cul7*$^{-/-}$ mice

Phenotype	Mouse type	
	Fbxw8$^{-/-}$	*Cul7*$^{-/-}$
Survival	Embryonic death (partial) Reduced size	Neonatal death Reduced size
Placenta	Abnormal development of spongiotrophoblast Smaller maternal vessel area in labyrinth	Abnormal development of spongiotrophoblast Smaller maternal vessel area in labyrinth
Other organs	None	Lungs unable to inflate Hypodermal hemorrhage

from extraembryonic ectoderm differentiate into syncytiotrophoblasts to form the labyrinth in concert with fetal blood vessels, and ectoplacental cone cells develop into spongiotrophoblasts (1, 8–10, 32). The labyrinth is essential for gas exchange and nutrition transfer between the maternal and fetal circulation (9, 10, 32). Our data now suggest that the Cul1-Fbxw8-Cul7 complex plays an essential role in the mid- to late stage of placental development, and that the embryonic death of *Fbxw8*$^{-/-}$ mice results from inappropriate development of the placenta. The less severe placental phenotype of *Cul7*$^{-/-}$ mice, compared with that of *Fbxw8*$^{-/-}$ mice, might be attributable to residual expression of Fbxw8 in *Cul7*$^{-/-}$ mice. In contrast, the maternal decidua and trophoblast giant cells appeared unaffected in *Fbxw8*$^{-/-}$ mice, whereas *Cul7*$^{-/-}$ mice exhibit a reduced number of trophoblast giant cells and an underdeveloped decidual layer (4), suggesting that Cul7 contributes to the growth of trophoblast giant cells and differentiation of the maternal decidua in an Fbxw8-independent manner.

All *Cul7*$^{-/-}$ mice die soon after birth from respiratory distress (4). In addition, ~20% of *Cul7*$^{-/-}$ mice exhibit hypodermal hemorrhage at late gestational ages (4). These phenotypes were not observed in *Fbxw8*$^{-/-}$ mice, again suggesting that Cul7 has Fbxw8-dependent and -independent functions. The latter functions might be mediated by substrate recognition subunits other than Fbxw8 that associate with Cul7 to form an E3 ligase or by ubiquitylation-independent activity of Cul7. Cul7 was originally identified as a binding partner for the large T antigen of simian virus 40, and it contains a BH3 domain in its COOH-terminal region, implicating Cul7 in cellular transformation and apoptosis (2, 24, 36). The phenotypic differences between *Fbxw8*$^{-/-}$ mice and *Cul7*$^{-/-}$ mice are thus likely attributable to the different expression patterns of the corresponding proteins and to Cul7-specific functions not related to Fbxw8-mediated ubiquitylation.

ACKNOWLEDGMENTS

We thank Y. Shinomiya, K. Shinohara, N. Nishimura, R. Mitsuyasu, Y. Yoshimura, and other laboratory members for technical assistance; Y. Yamada for generating knockout mice; and A. Ohta for help in preparation of the manuscript.

This work was supported in part by a grant from the Ministry of Education, Culture, Sports, Science, and Technology of Japan and by a research grant from the Human Frontier Science Program.

REFERENCES

1. **Adamson, S. L., Y. Lu, K. J. Whiteley, D. Holmyard, M. Hemberger, C. Pfarrer, and J. C. Cross.** 2002. Interactions between trophoblast cells and the maternal and fetal circulation in the mouse placenta. Dev. Biol. **250:** 358–373.
2. **Ali, S. H., J. S. Kasper, T. Arai, and J. A. DeCaprio.** 2004. Cul7/p185/p193 binding to simian virus 40 large T antigen has a role in cellular transformation. J. Virol. **78:**2749–2757.
3. **Anson-Cartwright, L., K. Dawson, D. Holmyard, S. J. Fisher, R. A. Lazzarini, and J. C. Cross.** 2000. The glial cells missing-1 protein is essential for branching morphogenesis in the chorioallantoic placenta. Nat. Genet. **25:** 311–314.
4. **Arai, T., J. S. Kasper, J. R. Skaar, S. H. Ali, C. Takahashi, and J. A. DeCaprio.** 2003. Targeted disruption of p185/Cul7 gene results in abnormal vascular morphogenesis. Proc. Natl. Acad. Sci. USA **100:**9855–9860.
5. **Bessho, Y., R. Sakata, S. Komatsu, K. Shiota, S. Yamada, and R. Kageyama.** 2001. Dynamic expression and essential functions of Hes7 in somite segmentation. Genes Dev. **15:**2642–2647.
6. **Cardozo, T., and M. Pagano.** 2004. The SCF ubiquitin ligase: insights into a molecular machine. Nat. Rev. Mol. Cell. Biol. **5:**739–751.
7. **Cenciarelli, C., D. S. Chiaur, D. Guardavaccaro, W. Parks, M. Vidal, and M. Pagano.** 1999. Identification of a family of human F-box proteins. Curr. Biol. **9:**1177–1179.
8. **Cross, J. C.** 2005. How to make a placenta: mechanisms of trophoblast cell differentiation in mice–a review. Placenta **26:**S3–9.
9. **Cross, J. C., D. Baczyk, N. Dobric, M. Hemberger, M. Hughes, D. G. Simmons, H. Yamamoto, and J. C. Kingdom.** 2003. Genes, development and evolution of the placenta. Placenta **24:**123–130.
10. **Cross, J. C., M. Hemberger, Y. Lu, T. Nozaki, K. Whiteley, M. Masutani, and S. L. Adamson.** 2002. Trophoblast functions, angiogenesis and remodeling of the maternal vasculature in the placenta. Mol. Cell. Endocrinol. **187:**207–212.
11. **Dias, D. C., G. Dolios, R. Wang, and Z. Q. Pan.** 2002. CUL7: a DOC domain-containing cullin selectively binds Skp1.Fbx29 to form an SCF-like complex. Proc. Natl. Acad. Sci. USA **99:**16601–16606.
12. **Furukawa, M., Y. J. He, C. Borchers, and Y. Xiong.** 2003. Targeting of protein ubiquitination by BTB-Cullin 3-Roc1 ubiquitin ligases. Nat. Cell Biol. **5:**1001–1007.
13. **Guardavaccaro, D., and M. Pagano.** 2004. Oncogenic aberrations of cullin-dependent ubiquitin ligases. Oncogene **23:**2037–2049.
14. **Hashizume, R., M. Fukuda, I. Maeda, H. Nishikawa, D. Oyake, Y. Yabuki, H. Ogata, and T. Ohta.** 2001. The RING heterodimer BRCA1-BARD1 is a ubiquitin ligase inactivated by a breast cancer-derived mutation. J. Biol. Chem. **276:**14537–14540.
15. **Hatakeyama, S., M. Kitagawa, K. Nakayama, M. Shirane, M. Matsumoto, K. Hattori, H. Higashi, H. Nakano, K. Okumura, K. Onoe, R. A. Good, and K. I. Nakayama.** 1999. Ubiquitin-dependent degradation of IκBα is mediated by a ubiquitin ligase Skp1/Cul 1/F-box protein FWD1. Proc. Natl. Acad. Sci. USA **96:**3859–3863.
16. **Hershko, A., and A. Ciechanover.** 1998. The ubiquitin system. Annu. Rev. Biochem. **67:**425–479.
17. **Hicke, L.** 2001. Protein regulation by monoubiquitin. Nat. Rev. Mol. Cell. Biol. **2:**195–201.
18. **Huber, C., D. Dias-Santagata, A. Glaser, J. O'Sullivan, R. Brauner, K. Wu, X. Xu, K. Pearce, R. Wang, M. L. Uzielli, N. Dagoneau, W. Chemaitilly, A. Superti-Furga, H. D. Santos, A. Megarbane, G. Morin, G. Gillessen-Kaesbach, R. Hennekam, I. V. Burgt, G. C. Black, P. E. Clayton, A. Read, M. L. Merrer, P. J. Scambler, A. Munnich, Z. Q. Pan, R. Winter, and V. Cormier-Daire.** 2005. Identification of mutations in CUL7 in 3-M syndrome. Nat. Genet. **37:**1119–1124.
19. **Imai, Y., M. Soda, and R. Takahashi.** 2000. Parkin suppresses unfolded protein stress-induced cell death through its E3 ubiquitin-protein ligase activity. J. Biol. Chem. **275:**35661–35664.
20. **Jin, J., T. Cardozo, R. C. Lovering, S. J. Elledge, M. Pagano, and J. W. Harper.** 2004. Systematic analysis and nomenclature of mammalian F-box proteins. Genes Dev. **18:**2573–2580.
21. **Kamura, T., T. Hara, M. Matsumoto, N. Ishida, F. Okumura, S. Hatakeyama, M. Yoshida, K. Nakayama, and K. I. Nakayama.** 2004. Cytoplasmic ubiquitin ligase KPC regulates proteolysis of p27^{Kip1} at G1 phase. Nat. Cell Biol. **6:**1229–1235.
22. **Kamura, T., K. Maenaka, S. Kotoshiba, M. Matsumoto, D. Kohda, R. C. Conaway, J. W. Conaway, and K. I. Nakayama.** 2004. VHL-box and SOCS-box domains determine binding specificity for Cul2-Rbx1 and Cul5-Rbx2 modules of ubiquitin ligases. Genes Dev. **18:**3055–3065.
23. **Kipreos, E. T., and M. Pagano.** 2000. The F-box protein family. Genome Biol. **1:**REVIEWS3002.
24. **Kohrman, D. C., and M. J. Imperiale.** 1992. Simian virus 40 large T antigen stably complexes with a 185-kilodalton host protein. J. Virol. **66:**1752–1760.
25. **Kominami, K., I. Ochotorena, and T. Toda.** 1998. Two F-box/WD-repeat proteins Pop1 and Pop2 form hetero- and homo-complexes together with cullin-1 in the fission yeast SCF (Skp1-Cullin-1-F-box) ubiquitin ligase. Genes Cells **3:**721–735.
26. **Nakayama, K., N. Ishida, M. Shirane, A. Inomata, T. Inoue, N. Shishido, I. Horii, D. Y. Loh, and K. I. Nakayama.** 1996. Mice lacking p27^{Kip1} display increased body size, multiple organ hyperplasia, retinal dysplasia, and pituitary tumors. Cell **85:**707–720.
27. **Nakayama, K., H. Nagahama, Y. A. Minamishima, M. Matsumoto, I. Nakamichi, K. Kitagawa, M. Shirane, R. Tsunematsu, T. Tsukiyama, N. Ishida, M. Kitagawa, K. I. Nakayama, and S. Hatakeyama.** 2000. Targeted disruption of Skp2 results in accumulation of cyclin E and p27^{Kip1}, polyploidy and centrosome overduplication. EMBO J. **19:**2069–2081.
28. **Nakayama, K. I., and K. Nakayama.** 2005. Regulation of the cell cycle by SCF-type ubiquitin ligases. Semin. Cell Dev. Biol. **16:**323–333.
29. **Nikolaev, A. Y., M. Li, N. Puskas, J. Qin, and W. Gu.** 2003. Parc: a cytoplasmic anchor for p53. Cell **112:**29–40.
30. **Petroski, M. D., and R. J. Deshaies.** 2005. Function and regulation of cullin-RING ubiquitin ligases. Nat. Rev. Mol. Cell. Biol. **6:**9–20.
31. **Pintard, L., J. H. Willis, A. Willems, J. L. Johnson, M. Srayko, T. Kurz, S. Glaser, P. E. Mains, M. Tyers, B. Bowerman, and M. Peter.** 2003. The BTB protein MEL-26 is a substrate-specific adaptor of the CUL-3 ubiquitin-ligase. Nature **425:**311–316.
32. **Rossant, J., and J. C. Cross.** 2001. Placental development: lessons from mouse mutants. Nat. Rev. Genet. **2:**538–548.

33. **Seibert, V., C. Prohl, I. Schoultz, E. Rhee, R. Lopez, K. Abderazzaq, C. Zhou, and D. A. Wolf.** 2002. Combinatorial diversity of fission yeast SCF ubiquitin ligases by homo- and heterooligomeric assemblies of the F-box proteins Pop1p and Pop2p. BMC Biochem. **3:**22.
34. **Skaar, J. R., T. Arai, and J. A. Decaprio.** 2005. Dimerization of CUL7 and PARC is not required for all CUL7 functions and mouse development. Mol. Cell. Biol. **25:**5579–5589.
35. **Suzuki, H., T. Chiba, T. Suzuki, T. Fujita, T. Ikenoue, M. Omata, K. Furuichi, H. Shikama, and K. Tanaka.** 2000. Homodimer of two F-box proteins βTrCP1 or βTrCP2 binds to IκBα for signal-dependent ubiquitination. J. Biol. Chem. **275:**2877–2884.
36. **Tsai, S. C., K. B. Pasumarthi, L. Pajak, M. Franklin, B. Patton, H. Wang, W. J. Henzel, J. T. Stults, and L. J. Field.** 2000. Simian virus 40 large T antigen binds a novel Bcl-2 homology domain 3-containing proapoptosis protein in the cytoplasm. J. Biol. Chem. **275:**3239–3246.
37. **Tsunematsu, R., K. Nakayama, Y. Oike, M. Nishiyama, N. Ishida, S. Hatakeyama, Y. Bessho, R. Kageyama, T. Suda, and K. I. Nakayama.** 2004. Mouse Fbw7/Sel-10/Cdc4 is required for notch degradation during vascular development. J. Biol. Chem. **279:**9417–9423.
38. **Weissman, A. M.** 2001. Themes and variations on ubiquitylation. Nat. Rev. Mol. Cell. Biol. **2:**169–178.
39. **Winston, J. T., D. M. Koepp, C. Zhu, S. J. Elledge, and J. W. Harper.** 1999. A family of mammalian F-box proteins. Curr. Biol. **9:**1180–1182.
40. **Xu, L., Y. Wei, J. Reboul, P. Vaglio, T. H. Shin, M. Vidal, S. J. Elledge, and J. W. Harper.** 2003. BTB proteins are substrate-specific adaptors in an SCF-like modular ubiquitin ligase containing CUL-3. Nature **425:**316–321.